IEEE Access
Multidisciplinary | Rapid Review | Open Access Journal

Received July 27, 2019, accepted August 8, 2019, date of publication August 21, 2019, date of current version September 5, 2019.

Digital Object Identifier 10.1109/ACCESS.2019.2936606

Bayesian Optimization for Multimodal Heterogeneous Network Orchestration via Hybrid Probability Process

HAI WANG[1], GENG ZHANG[2], HAO JIANG[1], JING WU[1], XING YANG[1], AND MO ZHOU[1]
[1]Electronic Information School, Wuhan University, Hubei 430000, China
[2]China Electric Power Research Institute, Beijing 100192, China

Corresponding author: Hao Jiang (jh@whu.edu.cn)

This work was supported in part by the Project of State Grid Corporation of China, in 2017, and in part by the Research on Simulation Model and Simulation Method of Power Communication System under Grant XX71-17-006.

ABSTRACT In the era of 5G and beyond, heterogeneous network orchestration has become a tremendous issue. The dilemma facing future systems is how to allocate integrated resources to satisfy multifarious services, which is an imperative but arduous task in forming a systematic mathematical model and quantifying the model with its multi-layer uncertainty characteristics. Aiming at the statistical representation and optimization in multimodal heterogenous networks for 5G and beyond, we propose a novel hybrid probability process (HPP) as a generalized surrogate model and a weighted degenerated upper confidence bound (WDUCB) criterion for Bayesian optimization (BO). We apply the proposed HPP-WDUCB combination to our developed simulation platform and configure several applications of the integration of space information network in next generation communication systems. And we compared the proposed method with other surrogate models and acquisition strategies from a range of perspectives. The experiment results yield significant applicability and excellent performance in multimodal system representation and optimization which provides an effective statistical modeling and orchestration references for network tuning.

INDEX TERMS Bayesian optimization, heterogeneous network orchestration, 5G and beyond, hybrid probability process, weight degenerate upper confidence bound.

I. INTRODUCTION

Information network technological innovation with wireless architectural evolution has been flourishing in the past few decades. The widespread proliferation of coexisting heterogeneous networks, which are oriented by different network providers and network architectures with a large number of heterogeneous applications, as well as sparse features and disparate users, has been experienced [1].

Specifically, focusing on 5G and beyond communication systems, heterogeneous network orchestration has become a tremendous issue as the orientation of technology of the next-generation information society in the next decade. However, it is difficult to integrate and utilize resources between contrasting sub-systems. Due to the high complexity and uncertainty of multimodal heterogeneous networks themselves and the sparse and bursty nature of potential users' personalized services, the potential indicators of heterogeneous systems are intertwined. The design elements in the specific multi-service scenarios are intermingled and decrease the system efficiency and the users' quality of service (QoS).

In general, network modeling and optimization through mathematical models are extremely costly, and these models work only under ideal conditions with strong hypotheses. To address this quantity dilemma, we obtained inspiration from the Bayesian posterior method, and we introduced sequential model Bayesian optimization [2] as a global optimization method that widely emerges in these myriad of orchestration problems. The general method provides a way to estimate the optimal design by greedy iteration strategies with generic agents [3]. However, the initial proxy model cannot be reasonably applied to act as a surrogate model of most heterogeneous network systems with composite multimodal features and leads to anonymous fitting failure during network orchestration.

The associate editor coordinating the review of this article and approving it for publication was Mauro Fadda.

In this paper, to combine a universal representation of heterogeneous networks implying a relationship between system performance indicators and design elements with the optimization of multi-service schemes in 5G and beyond, our main contributions can be summarized as follows:

1) A novel hybrid probability process (HPP) surrogate model is proposed. The intermediate features of the cluster procedure are included in the final fitting process, and we optimize the computational complexity with an approximate calculation and feature extraction approach. The proposed HPP model can be treated as a generalized multimodal extension of the Gaussian mixture distribution with a sequential stochastic process.

2) To fit the structure of the HPP model, we combine the convergence weight with the exploration-exploitation strategy. A hyperparameter insensitive weighted degenerate upper confidence bound (WDUCB) criterion is guaranteed, and we design a well-balanced strategy to control the iteration under a small computational complexity.

3) From the above proposal, a distributed network simulation platform and a self-configuring HPP-based Bayesian optimization iterative process module are established. We apply the module to a typical multi-service application scenario of 5G and next-generation systems to integrated LEO satellite communication constellation and remote sensing systems in different design dimensions. Compared with several primitive method combinations, the results are shown to exhibit the gains of our proposed model from multiple perspectives.

The remainder of this paper is organized as follows. In Section II, a brief overview of the architecture design and development of heterogeneous networks and the development and restriction of Bayesian optimization are discussed. The design and fitting process of the hybrid probability process model with weight degenerate upper confidence bound criterion for multimodal heterogeneous network systems is given in detail in Section III. Section IV describes the specific use case scenario, and experimental results are provided. The conclusion follows in Section V.

II. RELATED WORKS

A. HETEROGENEOUS NETWORKS

With the rapid development of mobile communication networks and Internet technology, mobile communication generations are advancing approximately every 10 years [4]. For 5G and beyond, a large number of different heterogeneous information networks have emerged. Users are exposed to a complex heterogeneous resource environment. The significance of information acquisition and transmission and the importance of resource efficiency and allocation mechanisms have changed greatly.

From a terrestrial perspective, research is mainly aimed at different types of information system resource integrations and service reliability between different communication regularities. The concept of heterogeneous networks can be traced back to the 1970s, from the integration of services to the concept of Next-Generation Network (NGN) [5] to the end of the last century; this is the first time the prospect of heterogeneous information network convergence based on unified IP technology has been presented. The BRAIN project proposes an open architecture for the integration of a wireless local area network (WLAN) and a general mobile communication system (UMTS) [6]. The Ambient Network project (AN) [7] was a large-scale cooperative project under the Sixth Framework Plan of the European Union; its goal is to promote effective interconnection between wireless network collaborators. The Mobile and wireless communications Enablers for the Twenty-twenty Information Society (METIS) [8] project envisions a 5G system concept that efficiently integrates new applications developed in the METIS horizontal topics and evolves versions of existing services and systems. Some early efforts have been dedicated to HetNets [9] to satisfy these more stringent demands.

Concerning the other prospect within space segment, the next generation of mobile communication has strived to achieve full coverage of the time and space dimensions [10], therein providing services with high-efficiency spectrum sharing and multi-access assurance. The objectives and characteristics of space-terrestrial integrated systems are summarized [11]. Some newly featured architectures attempt to satisfy the requirements for terrestrial-mobile and space-satellite systems (TMSs) [12] in future networks. These topics correspond to not only the network transmission function but also the cooperation of collaborative services [13], thus providing efficient service mechanisms for applications in the next generation of space information networks. Aiming at the integration of pointing, navigating, timing, remote sensing, and communication resources, a novel architecture for a space resource integrated information platform was proposed in 2015 [14] for the enhancement of basic mission protection. For the era of 5G and beyond, multiple network standards, such as long-term evolution advanced (LTE-A) [15], the green network [16] and network-2030 [17], have been proposed and will coexist with each other for a period of time.

We need to find an appropriate pattern to build optimized heterogeneous services; however, this issue is rarely the subject of attention. Current researchers primarily focus on mathematical model analysis and resource allocation at the technical level for a specific case. Most currently proposed converged networks only remain at the architecture design stages, therein neglecting the impact of future service resource scheduling and the complex orchestration of heterogeneous networks. A lack of a universal approach to the model representation of heterogeneous network performance at the system level exists. Therefore, we introduce the Bayesian optimization method for systematic heterogeneous research.

B. BAYESIAN OPTIMIZATION

Bayesian optimization is a powerful tool for the joint optimization of design choices and has gained substantial

popularity in recent years. As a global model-free optimization algorithm, the objective of BO is to build the surrogate model and find the global optimal solution of the following formula.

$$x^* = argmax_{x \in A \in R^d} f(x) \tag{1}$$

The framework of a typical BO consists of two core parts: a surrogate model and an acquisition function. Through the Bayesian posterior probability formula, the surrogate model is used as an agent for the black-box function, while the acquisition function is provided to balance the criterion for searching the query point through iteration. In contrast to other model-free global optimization methods, BO utilizes prior knowledge and a weak hypothesis, and it constructs the surrogate agent with minimal cost [2].

Bayesian optimization-based methods are effectively used to solve the problem of orchestration and optimization in decision theory. Companies such as Google and Microsoft use BO technology to recommend news articles to subscribers based on the content of their websites, videos, music, etc [18]. Bergstra *et al.* used BO to automatically adjust the hyperparameters of neural networks and deep belief networks [19] [20]. Snoek *et al.* used Bayesian optimization to automatically adjust the hyperparameters in convolutional neural networks [21]. Mahendran *et al.* proposed an adaptive Markov chain Monte Carlo algorithm based on Bayesian Optimization [22]. Thornton *et al.* applied BO to propose an automatic model selection and hyperparameter adjustment method for the Auto-WEKA classification algorithm [23]. Wang *et al.* improved the efficiency of the solver by adjusting the parameters of the mixed integer programming solver through Bayesian optimization [24]. Xia *et al.* used Bayesian optimization to adjust the super-parameters in a decision tree to improve the accuracy of credit evaluation [25], and Klein *et al.* proposed a fast Bayesian optimization method that can adjust the hyperparameters of machine learning algorithms on large-scale datasets [26]. Zhang *et al.* used a Bayesian optimization-based peak searching algorithm for clustering in wireless sensor networks to optimize the sensor position [27]. Candelieri *et al.* used Bayesian optimization in water distribution systems to operation pump systems [28]. Deepmind proposed conditional neural processes (CNPs) combined with a stochastic process with deep neural networks to obtain the benefits of both methods [29]. Obviously, BO has become a mainstream approach in the fields of artificial intelligence, robotics, industrial manufacturing, etc.

Bayesian optimization shows remarkable prospects in a wide range of engineering applications. Machines can predict future data according to the probability framework and make decisions based on the predicted data. Ghahramani notes that Bayesian optimization is one of the most advanced and promising technologies in probabilistic machine learning and artificial intelligence [3]. However, from the system model perspective, typical Bayesian optimization does not solve the problem of the credibility of the expression of an uncertain function. Simultaneously, in specific multi-modal system environments, particularly heterogeneous networks, the original BO surrogate model is not applicable.

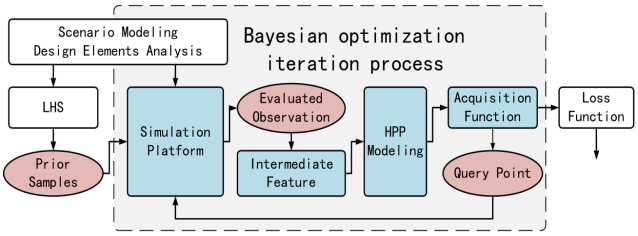

FIGURE 1. The iteration process for heterogeneous networks.

III. METHODS

A. A GENERAL SEQUENTIAL BAYESIAN OPTIMIZATION FOR HETEROGENEOUS NETWORKS SCHEME

We start with the limitations mentioned above. In this section, we detail a universal Bayesian optimization approach for uncertainty modeling and a sequential optimization paradigm for the multimodal heterogeneous network representation with optimization. As the core part of the optimization system shown in the frame in Fig. 1.

To escape from the ambiguous and inordinate cost in a specific theoretical model, we adapt the method to general heterogeneous network multi-service scenarios embedded into network simulations. The proposed iteration process controls the direction of the system parameter design.

Individually, we introduce the novel hybrid probability process (HPP) model and weighted degenerate upper confidence bound (WDUCB) criterion into the iteration process. The Latin hyperspace sampling (LHS) method [30] is applied to select the prior observations. Therefore, we obtain the prior train data and characteristics from the statistics of the system distribution. We rebuild the posterior surrogate model by fitting the performance appraisal of a specific scenario. The general procedure for the uncertainty analysis and optimization of heterogeneous network scenarios is as follows:

1) We chose the design elements x and performance parameters y in the specified scenarios.

2) We pre-sample from the element dimension using LHS and obtain the prior observations by simulation.

3) We apply the HPP surrogate model fitting process.

4) The WDUCB acquisition function chooses the optimal combination of design parameters (query point).

5) We set the loss function, and the query points are fed back to the simulation component. The new posterior observations are used to update the surrogate model, and the process iterates from step 3 to step 4.

6) After the cost function reaches the threshold, the iteration is stopped, and we obtain the optimized estimation and the representation model of the heterogeneous systems.

B. HYBRID PROBABILITY PROCESS

Considering a general multimodal hybrid probability process model applicable to key components for the sequential BO method, we propose a novel hybrid probability process

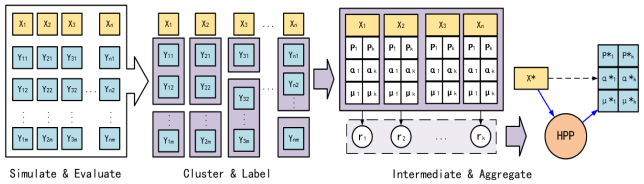

FIGURE 2. The fitting process of hybrid probability process.

model. In our weak hypothesis, the parameter dimension of the system is finite and sequential. The fitting process is shown in Fig. 2.

Just as the Gaussian process can be seen as an extension of the multivariate Gaussian distribution, we envisage the hybrid probability process as the extension of the multivariate Gaussian mixture distribution over the variables, and we aggregate the detailed distribution information into the stochastic process. The basic component unit in the mixed distribution can generally be any distribution. Considering the calculation cost of the hybrid model and the applicability of the features, we choose the Gaussian probability distribution as the meta-component, and the distribution features of the raw data can be fine grained and easily obtained.

Combining the mixture distribution model with the stochastic process, the mixture distribution is used over the specified random variable, with a variable combination x, and the Gaussian mixture model can be written as follows:

$$p(x) = \sum_{k=1}^{K} \rho_k \emptyset(x|\mu_k, \sigma_k^2) \tag{2}$$

The $\emptyset(x|\mu_k, \sigma_k^2)$ denotes the k-th cluster of the distribution component in the mixture model.

ρ_k corresponds to the weight of each component. Thus, $\emptyset(x|\mu_k, \sigma_k^2)$ can be expressed as the specific probability distribution function form:

$$\emptyset(x|\mu_k, \sigma_k^2) = \frac{1}{\sqrt{2\pi}\sigma_k} exp\left[-\frac{(x-\mu_k)^2}{2\sigma_k^2}\right] \tag{3}$$

The Gaussian mixture model is composed of several Gaussian distributions, which can accurately represent a complex probability distribution. Meanwhile, the intermediate features are extracted for subsequent modeling.

As the observation dataset

$$D_{1:t} = \{(x_1, y_1), (x_2, y_2), \ldots, (x_t, y_t)\} \tag{4}$$

x_t denotes the t-th parameter combination of the design, $x_t = \{x_1, x_2, \ldots, x_n\}$. For the vector x_t, x_n is the n-th element of x_t.

y_t denotes the collected observation data of the exact x_t, where $y_t = \{y_{t1}, y_{t2}, \ldots, y_{tm}\}$. For the y_t, y_{tm} represents the m-th observation of x_t. Therefore, under each design combination x, we need to use the observation points y_t to obtain the characteristics of the network performance.

With the influence of the implicit variables ρ_k, the expected maximum clustering algorithm is adapted to iteratively fit the model. Generally, we suppose that the mixture distribution has k components to find the implicit category z of each sample in $D_{1:t}$, and $p(y, z)$ can be maximized. The maximum likelihood estimates of $p(y, z)$ are as follows:

$$l(\theta) = \sum_{i=1}^{m} \log p(y_{ti}; \theta) = \sum_{i=1}^{m} log \sum_{z} p(y_{ti}, z; \theta) \tag{5}$$

Let $Q_j(z)$ be the distribution of the implicit variable z; thus,

$$\sum_{j=1}^{z} Q_j(z) = 1, \quad 0 \le Q_j(z) \le 1 \tag{6}$$

The following formulas can be derived from the previous explanations:

$$\sum_{i=1}^{m} \log p(y_{ti}; \theta) = \sum_{i=1}^{m} log \sum_{z^i} p\left(y_{ti}, z^i; \theta\right) \tag{7}$$

$$= \sum_{i=1}^{m} log \sum_{z^i} Q_i\left(z^i\right) \frac{p\left(y_{ti}, z^i; \theta\right)}{Q_i\left(z^i\right)} \tag{8}$$

$$\ge \sum_{i=1}^{m} \sum_{z^i} Q_i\left(z^i\right) log \frac{p\left(y_{ti}, z^i; \theta\right)}{Q_i\left(z^i\right)} \tag{9}$$

The origin of the above inequalities lies in the Jensen inequalities. Hence, the likelihood function's lower bound is found considering that, in the Gaussian mixture model, w_j^i means the probability that the observation y_{ti} belongs to the j-th cluster as follows: $w_j^i = Q_i\left(z^i = j\right) = p\left(z^i = j | y_{ti}; \theta_j\right)$.

Thus, we fix $Q_i\left(z^i\right)$ and maximize $l(\theta)$ as follows:

$$\sum_{i=1}^{m} \sum_{z^i} Q_i\left(z^i\right) log \frac{p\left(y_{ti}, z^i; \theta\right)}{Q_i\left(z^i\right)} \tag{10}$$

$$= \sum_{i=1}^{n} \sum_{j=1}^{k} Q_i\left(z^i = j\right) log \frac{p\left(y_{ti}, z^i = j; \theta_j\right) p\left(z^i = j; \theta_j\right)}{Q_i\left(z^i = j\right)} \tag{11}$$

θ_j indicates the characteristics of the mixture distribution parameters $\theta_j = \left(\rho_j, \mu_j, \sigma_j^2\right)$, while

$$= \sum_{i=1}^{m} \sum_{j=1}^{k} w_j^i log \frac{\frac{1}{\sqrt{2\pi}\sigma_j} exp\left[-\frac{(x-\mu_j)^2}{2\sigma_j^2}\right] \rho_j}{w_j^i}$$

Fixing variables to derive μ, we obtain the iterative objective function of μ:

$$\mu_j = \frac{\sum_{i=1}^{n} w_j^i y_{ti}}{\sum_{i=1}^{n} w_j^i} \tag{12}$$

For ρ_j, the formulas can be optimized as follows:

$$\sum_{i=1}^{n} \sum_{j=1}^{k} w_j^i log \rho_j \tag{13}$$

Consider Lagrange multipliers and the constraint of ρ_j, which can be expressed as follows:

$$\rho_j = \frac{1}{m} \sum_{i=1}^{m} w_j^i \tag{14}$$

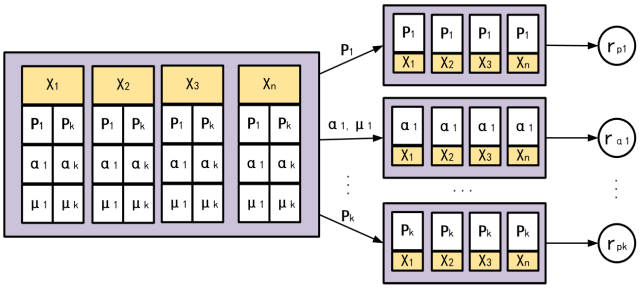

FIGURE 3. The intermediate process.

Thus, the iterative objective function of σ_j^2 becomes

$$\sigma_j^2 = \frac{\sum_{i=1}^{m} w_j^i \left(y_{ti} - \mu_j\right)\left(y_{ti} - \mu_j\right)}{\sum_{i=1}^{m} w_j^i} \tag{15}$$

The algorithm detailed above is a soft clustering approach for general parameter estimation. Without any prior information, the label and probability for every observation oscillate during the iterative process. In brief, the soft clustering approach is more reasonable but more computationally expensive than the hard clustering algorithm. In certain cases, to reduce the computational cost of the iterative clustering process, hard clustering methods with a computationally improved approach are employed. The number of clusters and the other hyperparameters of intermediate distribution knowledge, such as the threshold of the kernel distance, can be guaranteed by the probabilistic statistical analysis of prior observations.

The intermediate clustering process greatly reduces the amount of raw data. The observations $D_{1:t}$ are abstracted into those distribution characteristics

$$I_{1:t} = \{(x_1, \theta_1), (x_2, \theta_2), \ldots, (x_t, \theta_t)\} \tag{16}$$

in which

$$\theta_t = \{\theta_{t1}, \theta_{t2}, \ldots, \theta_{tz}\} \tag{17}$$

and $\theta_{tz} = \left(\rho_{tz}, \mu_{tz}, \sigma_{tz}^2\right)$ which is the z-th cluster of intermediate hybrid probability process elements.

We postulate that the probability distribution of the network performance between the adjacent combinations of design parameters is also relatively similar and weakly stable. A pair of observation points with smaller generalized distances can be expected to have a larger mutual influence. Therefore, to the hypothesis, we are able to construct the multivariate stochastic process for the labeled features of each cluster.

For the same tag $\left\{\left(x_1, \theta_{1j}\right), \left(x_2, \theta_{2j}\right), \ldots, \left(x_t, \theta_{tj}\right)\right\}$ of intermediate elements, here, θ_{tj} represents the t-th observation fitting features of the j-th basic component, where $1 \leq j \leq z$ represents the number of clusters for the structure of the intermediate element and intermediate process r, shown in Fig. 3.

To establish a mathematical connection between design combinations in the parameter space to simultaneously externalize the influence of system uncertainty noise on network performance, we compared different types of classifier prediction models.

The prediction by the artificial neural network (ANN) is accurate and credible in the case of a large amount of training observations. However, as a black-box model, the interpretability and system volatility expression of ANNs are poor; simultaneously, the structure of the ANN needs to be thoroughly designed, and many hyperparameters often need to be adjusted.

Conversely, the random forest (RF) does not require a large amount of tuning work; however, in the full parameter space, it is difficult to establish the uncertainty relationship between the design elements of the system. Typically in small hypercubes with fewer sample points, the accuracy of the prediction is not satisfactory.

The Gaussian process (GP) is based on the Bayesian conditional posterior probability, which is in contrast to the clustering features of the Gaussian mixture model, and it is easier to explain the uncertainty characteristics of the system. The Gaussian process can be treated as a normal distribution over a function, which can be expressed as follows:

$$f(x) \sim GP\left(m(x), k\left(x, x'\right)\right) \tag{18}$$

In the r fitting process, the $m(x)$ is usually set to 0, and the kernel $k\left(x, x'\right)$ is the core component usually considered as the covariance matrix of the kernel function to describe the conjunction between every observation point.

Simultaneously, the selection of kernel functions $k\left(x, x'\right)$ for the covariance matrix is remarkably determinant, being related to the smoothness of the process sampling and directly affecting the matching degree between the Gaussian process and the data properties. Here, we utilize the benefits of Matern kernels [3], which contains a smoothing coefficient τ:

$$k\left(x_i, x_j\right) = \frac{1}{2^{\tau-1}\Gamma(\tau)}\left(2\sqrt{\tau}\left|\left|x_i - x_j\right|\right|\right)^{\tau} H_{\tau} \times \left(2\sqrt{\tau}\left|\left|x_i - x_j\right|\right|\right) \tag{19}$$

$\Gamma(.)$ and $H(.)$ are the gamma function and Bessel function. When $\tau \to \infty$, the corresponding covariance function is also called the square exponential kernel or the Gaussian kernel, and the corresponding process is second-order differentiable everywhere and highly smooth.

Thus, for a set of training samples $X = (x_1, x_2, \ldots, x_t)$ and a set of corresponding observations $f_{1:t} = (f_1, f_2, \ldots, f_t)$, there exists a joint Gaussian distribution that satisfies $N(0, K)$:

$$K = \begin{bmatrix} k(x_1, x_1) & \ldots & k(x_1, x_t) \\ \ldots & \ldots & \ldots \\ k(x_t, x_1) & \ldots & k(x_t, x_t) \end{bmatrix} \tag{20}$$

where the K represents the covariance matrix of the observation $f_{1:t}$. With the set of prior sample combinations $\{x_{1:t}, f_{1:t}\}$, for a new sample, we assume the joint Gaussian distribution

of x_{t+1} as follows:

$$\begin{bmatrix} f_{1:t} \\ f_{t+1} \end{bmatrix} \sim N\left(0, \begin{bmatrix} K & k \\ k^T & k\left(x_{t+1}, x_{t+1}\right) \end{bmatrix}\right) \tag{21}$$

In addition,

$k = [k\left(x_{t+1}, x_1\right)\ k\left(x_{t+1}, x_2\right) \ldots\ k\left(x_{t+1}, x_t\right)]$

The posterior probability of f_{t+1} can be calculated by the above formula. We obtain the following:

$$P\left(f_{t+1}|x_{1:t+1}\right) = N\left(\mu_t\left(x_{t+1}\right), \sigma_t^2\left(x_{t+1}\right)\right) \tag{22}$$

$$\mu_t\left(x_{t+1}\right) = k^T K^{-1} f_{1:t} \tag{23}$$

$$\sigma_t^2\left(x_{t+1}\right) = k\left(x_{t+1}, x_{t+1}\right) - k^T K^{-1} k \tag{24}$$

Taking query samples from the design parameter dimension as x_{t+1}, the details, including the expected f_{t+1} with its confidence kernel measure, can be progressively predicted.

With the concentrated extracted features from the mixture distribution model, we first construct a covariance matrix with the extracted characteristic set $I_{1:t}$. We classify the intermediate features by the labels of the clusters and congregate the features $\sum_{n=1}^{t} \theta_{nj}\left(\rho_{nj}, \mu_{nj}, \sigma_{nj}^2\right)$ for each intermediate process r.

The input of the intermediate process is the training set of design parameter combinations $x_{1:t}$ with the features $\sum_{n=1}^{t} \theta_{nj}\left(\rho_{nj}, \mu_{nj}, \sigma_{nj}^2\right)$, and the output is the stochastic process over the function of the prospective performance appraisal based on the probability distribution. This can be expressed as $\mu_j(x) \sim r\left(m\left(\mu_j\right), k\left(x, x'\right)\right)$ and $\rho_j(x) \sim r\left(m\left(\rho_j\right), k\left(x, x'\right)\right)$. The aggregation process is shown in Fig. 4 for a component r.

Specifically, for the GP of the feature μ_j, the value oscillation σ_j^2 of the training set establishes the quantitative impact of system haphazardness and actually affects the autocorrelation elements of the samples. We introduce σ_j^2 to affect the result of the autocorrelation Kernel function, where the construction of the covariance matrix is tuned to the following:

$$K_{\mu_j}^* = \begin{bmatrix} k\left(x_1, x_1\right) + \sigma_{j1}^2 & \ldots & k\left(x_1, x_t\right) \\ \ldots & \ldots & \ldots \\ k\left(x_t, x_1\right) & \ldots & k\left(x_t, x_t\right) + \sigma_{jt}^2 \end{bmatrix} \tag{25}$$

The prediction is as follows:

$$\mu_t\left(x_{t+1}\right) = k^T K_{\mu_j}^{*-1} f_{1:t} \tag{26}$$

$$\sigma_{\mu_j}^2\left(x_{t+1}\right) = k\left(x_{t+1}, x_{t+1}\right) - k^T K_{\mu_j}^{*-1} k \tag{27}$$

After the intermediate process r of ρ_j and μ_j of each labeled feature set θ_{nj} is established, the new hybrid probability process model predicts the Gaussian mixed models of prior observations and expected representation distribution of the system in sequential parameter dimensions. As a widely applicable mixture distribution over a function, the hybrid probability process can be revealed by the pattern:

$$f(x) \sim HPP\left(x|r_{\rho_j}(x), r_{\alpha_j}(x)\right) \tag{28}$$

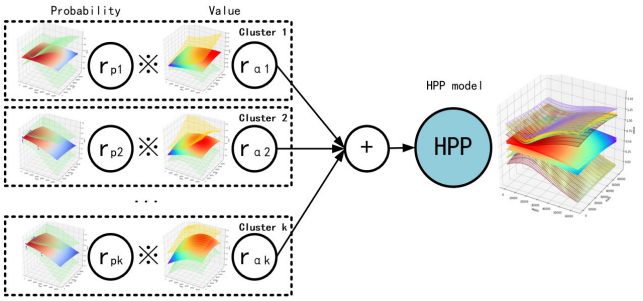

FIGURE 4. The aggregate process.

The intermediate component of the probability $r_{\rho_j}(x)$ indicates the probability distribution that the next query point assigns to this cluster j, and $r_{\alpha_j}(x)$ can be regarded as the expected performance appraisal distribution of the next query point in the j-th cluster as follows:

$$r_\rho(x|\rho, \sigma_\rho^2) \circledast r_\alpha(x|\alpha, \sigma_\alpha^2) = \sum_{j=1}^{z} r_{\rho_j}(x) * r_{\alpha_j}(x) \tag{29}$$

As shown in Fig. 4, $\circledast$ is considered the hybrid procedure of two corresponding stochastic processes. The multiplied distribution of the probability $r_{\rho_j}(x)$ with the expected value $r_{\alpha_j}(x)$ denotes the expected evaluation of the j-th component. The performance evaluation of the network is quantified from the perspective of clustering because this quantization is an evaluation distribution that retains the influence of the system's uncertainty noise. For the stochastic processes $\rho_j(x) \sim r_{\rho_j}(x|\alpha_{\rho x_j}, \sigma_{\rho x_j}^2)$ and $\alpha_j(x) \sim r_{\alpha_j}(x|\alpha_{\alpha x_j}, \sigma_{\alpha x_j}^2)$ of the j-th cluster, $\alpha_{\rho x_j}, \sigma_{\rho x_j}^2$ are the mean and variance of the j-th cluster probability ρ_j of x, and $\alpha_{\alpha x_j}$ and $\sigma_{\alpha x_j}^2$ represent the mean and variance of the j-th cluster's expected value α_j of x. Therefore, the multiplied distribution of the j-th expected evaluation obeys a Gaussian distribution:

$$\rho_j(x) * \alpha_j(x) \sim N(x|\mu_{x_j}, \sigma_{x_j}^2) \tag{30}$$

The feature distribution after multiplication is as follows:

$$N(x|\mu_{x_j}, \sigma_{x_j}^2) = \frac{S_{x_j}}{\sqrt{2\pi}\sigma_{x_j}} exp\left[-\frac{\left(\alpha_{\alpha_j} - \mu_{x_j}\right)^2}{2\sigma_{x_j}^2}\right] \tag{31}$$

Among them, the expectations of the j-th cluster values of x are

$$\mu_{x_j} = \frac{\alpha_{\alpha x_j}\sigma_{\rho x_j}^2 + \alpha_{\rho x_j}\sigma_{\alpha x_j}^2}{\sigma_{\rho x_j}^2 + \sigma_{\alpha x_j}^2} \tag{32}$$

$$\sigma_{x_j}^2 = \frac{\sigma_{\rho x_j}^2 \sigma_{\alpha x_j}^2}{\sigma_{\rho x_j}^2 + \sigma_{\alpha x_j}^2} \tag{33}$$

and the coefficient in the probability density function can be expanded to $S_{x_j} = \frac{1}{\sqrt{2\pi\left(\sigma_{\rho x_j}^2 + \sigma_{\alpha x_j}^2\right)}} exp\left[-\frac{\left(\alpha_{\alpha x_j} - \alpha_{\rho x_j}\right)^2}{2\left(\sigma_{\rho x_j}^2 + \sigma_{\alpha x_j}^2\right)}\right]$.

Thus,

$$r_\rho(x|\rho,\sigma_\rho^2) \circledast r_\alpha(x|\alpha,\sigma_\alpha^2) \sim N(x|\sum_{j=1}^{z}\mu_{x_j},\sum_{j=1}^{z}\sigma_{x_j}^2) \quad (34)$$

Theoretically, this provides an expression of the overall expected distribution of the heterogeneous system. If the number of clusters approaches infinity, $r_\rho(x|\rho,\sigma_\rho^2) \circledast r_\alpha(x|\alpha,\sigma_\alpha^2)$ will degenerate into the normal distribution of original observations, and the HPP model becomes a Gaussian process.

As an extension model of uncertainty-evaluated estimation with a collection of mixture distribution characteristics of observations, the HPP elegantly blends the impressive expressive ability of a mixed probability model into a lightweight structure with high flexibility and scalability. Compared with other prototype surrogate models, the HPP does not require a large amount of tuning work for the hyperparameters in the model. While ensuring the accuracy of the prediction, being in contrast to black-box models, such as neural networks, with poor interpretability, the hybrid probability distribution between the design and performance appraisal can also be interpreted and expressed in fine-grained detail. The kernel trick can alleviate the failures of each intermediate fitting process and the error of the acquisition strategy selection resulting from cold starts with a limited number of prior observations.

During the posterior modeling iteration, the most computationally intensive aspect of the fitting process is the construction of the kernel covariance matrix of the observation in the intermediate process. The computational complexity of the inversion process for the covariance matrix of n*n order is at least $O\left(n^3\right)$ in time and $O\left(n\right)$ in time for prediction on a query point [2], where the fitting process is affected by the volume of the prior training set. Simultaneously, the HPP is more compact than the single modality surrogate model, therein minimizing the computational complexity as much as possible. From the data volume perspective, the clustering and labelling processes extract intermediate features from obviously blocky prior observations to replace an enormous amount of raw data, reducing the size of the training data from $n * t$ of $D_{1:n}$ to $n * 2 * j$ of $I_{1:n}$, where $j \ll t$. From the fitting process perspective, the approximation algorithm for modeling can be adapted to these specific scenarios. We introduce sparse Gaussian processes using the pseudo-input (SPGP) [31] method into the aggregation procedure. During the covariance matrix fitting process, a pseudo-input can be used instead of the original parameter dimension, and rank reduction is carried out. This can reduce the computational complexity from $O\left(n^3\right)$ to $O\left(m^2n\right)$ for training and $O\left(m^2\right)$ for prediction, where $m \leq n$.

C. WEIGHTED DEGENERATE UPPER CONFIDENCE BOUND

Limited by realistic constraints of heterogeneous networks, the acquisition function must be considered with an agile framework and a broad range of applicability. Additionally, the strategy should take advantage of the posterior prediction from the proposed HPP, therein strongly considering the space exploration and model improvement in the iteration process. Comparing the mainstream acquisition criterion for the nonparametric surrogate model and inspired by the upper confidence bound (UCB) generally implemented in the field of recommend systems and the K-arms bandit problem, we propose a novel weight degenerate upper confidence bound (WDUCB) criterion for the HPP model.

Srinivas *et al.* proposed a Gaussian-process-based upper confidence bound (GP-UCB) strategy in 2010 [32]. The corresponding value of the UCB at an arbitrary point x is as follows:

$$UCB\left(x\right) = \mu_x + \beta\sigma_x^2 \quad (35)$$

The UCB criterion is a popular method of negotiation in exploration-and-exploitation (E-E) situations with provable cumulative regret bounds in exploration-and-exploitation problems [33]. The guiding principle behind this class of strategies is to be optimistic in the volume of the network uncertainty. For multimodal HPP, utilizing the aspect of clustering, the corresponding expected features of the j-th cluster are as follows:

$$\mu_{x_j} = \frac{\alpha_{\alpha x_j}\sigma_{\rho x_j}^2 + \alpha_{\rho x_j}\sigma_{\alpha x_j}^2}{\sigma_{\rho x_j}^2 + \sigma_{\alpha x_j}^2} \quad (36)$$

In addition,

$$\sigma_{x_j}^2 = \frac{\sigma_{\rho x_j}^2\sigma_{\alpha x_j}^2}{\sigma_{\rho x_j}^2 + \sigma_{\alpha x_j}^2} \quad (37)$$

Thus,

$$UCB\left(x\right) = \mu_x + \beta^T\sigma^2{}_x \quad (38)$$

where the number of clusters is z, $1 \leq j \leq z$, for arbitrary query points x, in which $\mu_x = \left[\mu_{x_1}, \mu_{x_2}, \ldots, \mu_{x_z}\right]$, $\sigma^2{}_x = \left[\sigma_{x_1}^2, \sigma_{x_2}^2, \ldots, \sigma_{x_z}^2\right]$, $\beta = [\beta_1, \beta_2, \ldots, \beta_z]$. Determined by the categorical β, the UCB criterion presents an enormous discrepancy in E-E situations.

To minimize the tuning work in hyperparameter setting and scheduling, we substitute a degenerate coefficient τ into β, which is associated with the number of iterations, where τ is considered as a linear attenuation $\tau = \frac{h-i}{h}$ or exponential factor $\tau = e^{-\frac{i}{h}}$. h represents the standard number of iterations, and i represents the current number of iterations. As the number of iterations increases, the criterion of the acquisition function changes from exploration to exploitation. A linear or exponential attenuation factor can also be considered and selected according to the disparate requirements on the attenuation rate in the given scenario.

Taking the influence of different subjective and objective uncertainties of different clusters in the general scenario on the performance of the heterogeneous network itself into account, for the difference clusters of x, we give constant

weights to and assume the predicted weight vector ω_x of x as follows:

$$\omega_x = \left[\omega_{x_1}, \omega_{x_2}, \ldots, \omega_{x_z}\right] \tag{39}$$

The weight ω_{x_j} for the UCB of each cluster is based on the feature $\sigma_{x_j}^2$ that

$$\omega_{x_j} = \frac{\sigma_{x_j}^{2(2\tau-1)}}{\sum_{j=1}^{z} \sigma_{x_j}^{2(2\tau-1)}} \tag{40}$$

The weight ω_{x_j} is conspicuous correlated with the current iteration. Theoretically, the predicted network appraisal with greater fluctuations should be better focused on determining hidden information in the exploration phase to ensure a flexible balance in ω_{x_j} according to the the preference criterion.

The WDUCB strategy is as follows:

$$WDUCB\,(x) = \omega_x^T \left(\mu_x + \tau\beta^T {\sigma^2}_x\right) \tag{41}$$

Thus, we obtain the utility evaluation of the query point x. The WDUCB criterion associates the advantage of the UCB with the HPP, therein providing an effective adaptive strategy that avoids heavy calculation work on the acquisition function and achieving an optimal regret loss.

IV. EXPERIMENTS AND ANALYSIS

In this section, we present the test scenarios of a particular multi-task application of a heterogeneous space information network system constructed to investigate the efficiency of the proposed HPP models with the general WDUCB criterion. The experiments compared different surrogate models with different acquisition criteria from a series of perspectives, and the results were obtained on a set of two different dimensions of the design indicator spaces: a simple visualization of the package size of the delivery of two different services (2D) in the global integration and a benchmark higher dimensional (9D) scenario of a multi-task application of the heterogeneous network.

A. EXPERIMENTS ENVIRONMENT

According to the current test functions, there are still some function values with exact outputs without complex distribution features and that cannot adapt our concerned issue; thus, we utilize the high-level architecture (HLA) distributed simulation platform based on the EXATA as the preliminary experimental environment shown in Fig. 5. The simulation platform is established to auto-configure specific network scenario based on general network elements and architectures of current typical models and protocols. The module combines the function of simulation, observation and evaluation for the network scheme incident response. After each simulation process for a specific scenario, we iterate the surrogate model and obtain the query point to configure the next iteration process in the BO module, which is the core constituent of the sequential HPP model iterations.

The scenarios that we are concerned about mainly focus on specific multi-service scenarios for remote sensing satellite data on-orbit processing and fast return services to evaluate and optimize the design elements of the application layer aspect, as shown in Fig. 5.

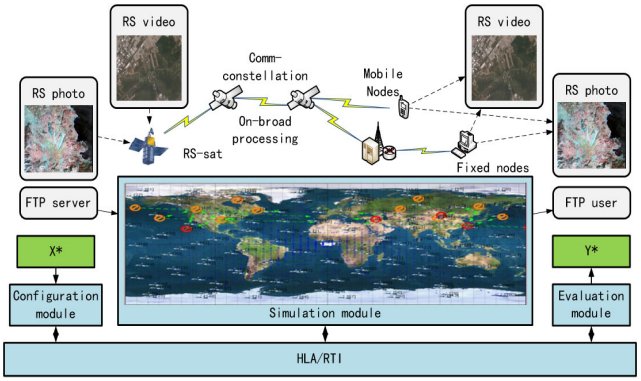

FIGURE 5. The structure of distributed simulation platform.

TABLE 1. Parameters setting.

Parameter	value	Parameter	value
Comm-sat	156	Comm-sat altitude	1050
Comm orbit	13	Comm in orbit	12
RS-sat	90	RS-sat altitude	860
RS orbit	6	RS in orbit	15
Comm phase diff	6	RS phase diff	2
Mobile node	40	Fixed node	60
Sat-Sat bandwidth	[1, 5]	Sat-User bandwidth	[30, 100]
IP protocol	OSPF,RIP,..	TCP buffer	[30, 65535]
VBR size	[0, 64000]	VBR interval	[0, 100]
Superapp size	[0, 64000]	Superapp interval	[0, 100]
Trafficgen size	[0, 64000]	Trafficgen interval	[0, 100]
...	...	...	...

The unit of Comm-sat and RS-sat altitude is Km, the unit of Sat-Sat bandwidth unit is G, the unit of sat-user bandwidth is M, the unit of package size is byte, interval unit is ms.

We build 13×12=156 broadband communication constellations (Comm-sat) and 15×6=90 LEO high-resolution remote sensing constellations (RS-sat). For the terrestrial system, we set 40 ground mobile nodes (aircraft, ships, mobile ground stations, etc.) and 60 fixed nodes (mainly fixed ground facility stations). The application flows from the data source to the user equipment, including RS video and image streams, which are generated by the Traffic-Generator (Trafficgen) and Superapplication (Superapp) flows in the EXATA application generator function module, as well as other Internet data streams treated as VBR flows, file transmission (FTP) services and noise. During every simulation iteration, 50 multi-aggregated flows are randomly generated.

The packet size, sending interval and service priorities of each type of application are optimized as the combination of design parameters, and the delay, jitter, throughput and packet loss rate of every flow's performance are evaluated by the evaluation module in the platform. With the AHP [34] evaluation appraisal as the evaluation value for the target and the above simulation model, we perform our experiments in 2D and 9D. Some of the scenario parameters are given in Table 1.

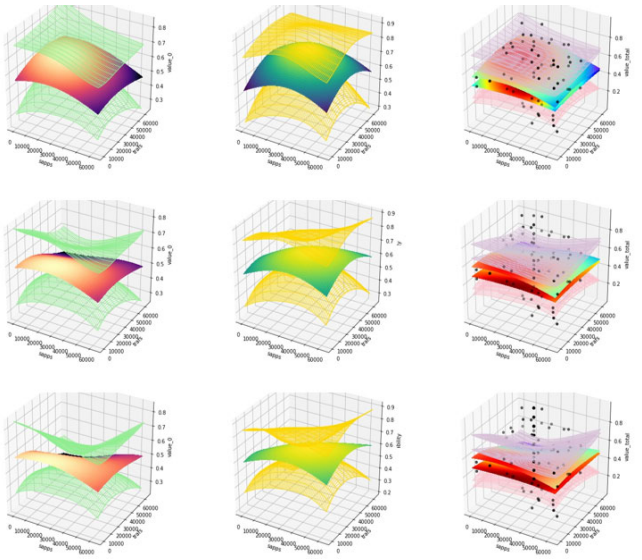

FIGURE 6. HPP diagram with 0 10 60 iterations.

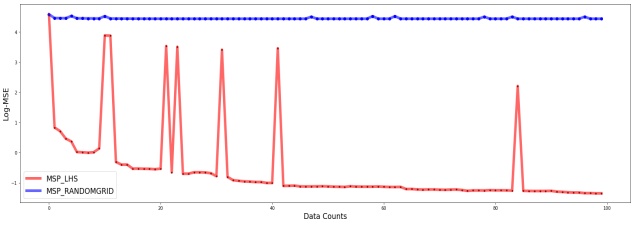

FIGURE 7. The MSE between two presampling methods.

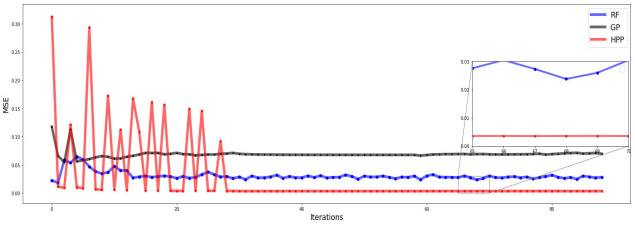

FIGURE 8. MSE in 2D.

B. RESULT ANALYSIS

1) ITERATION VISUALIZATION OF THREE-DIMENSIONAL FITTING PROCESS

Shown in Fig 6, the figure from left to right are the Gaussian process schematic diagram of the evaluation appraisal value and the expected probability of the first cluster, and the layer structure of the HPP model schematic diagram. The observations are given as the scatter in the layer structure.

With the iteration of the surrogate model, the observations are gradually fitted by the hybrid probability process. The results of the method appraisal will be explained in the following analysis.

2) COMPARISON OF PRIOR SAMPLE METHODS

The prior observations that we obtained in the high-dimensional space of the heterogeneous system are relatively scarce, while the surrogate model heavily relies on the distribution of the priori observation.

With the visualization of the HPP model, the posterior fitting result of the MSP model between the Latin hypercube sample method and the subjective authoritative design-based grid sampling observations can be determined from the thermodynamic diagram showing that the method of prior sampling for the observations has a significant influence on the surrogate model fitting process.

With the same prior observation amounts, as the amount of prior data gradually increases, as drawn in Fig. 7, With prior data increasing, the log-MSE of LHS is continuous decline. And the raw MSE of the HPP based on LHS converges to approximately 21% of the MSE of the HPP from the subjective authoritative design with grid sampling. In the above results, the LHS method can obtain a more reasonable and accurate prior surrogate model under the cold start condition of the small sample method.

TABLE 2. MSE in 2D.

iterations	1	2	5	10	30	50
HPP	0.31217	0.01157	0.00994	0.00681	0.00404	0.00379
RF	0.01118	0.02245	0.03028	0.02071	0.01382	0.01307
GP	0.31220	0.02934	0.02635	0.01793	0.01393	0.01294

3) COMPARISON OF SURROGATE MODELS IN ITERATIVE TEST

In this subsection, we compared the hybrid probability process with the Gaussian process and random forest to fit the simulation observations of the above-mentioned heterogeneous space information network scenarios.

The MSE, R-Squared, KL divergence and JS divergence are demonstrated to compare the performance of the surrogate models. The quantitative indicators of the MSE and R-Squared are calculated using the observation of the 2D parameters. The KL and JS divergences are calculated by the observation of the 9D parameters.

a: MSE

The MSE is a preliminary comparison indicator of the absolute error between the predicted and actual appraisal. As shown in Fig. 8, through the iteration and while continuously adding new knowledge, the indicator gradually is able to quantify the prediction error of the posterior model.

From these results, in the scenario with the 2D parameter space, the MSE index of RF is analogous to the GP, while the HPP's MSE is 29% of the GP's MSE on average after model convergence. The specific iteration data are given in Table 2.

In the high-dimensional application layer design parameter space scenario, the kernel function discrimination generalized distance becomes complicated due to the high-dimensional data. In the iterative process, the fitting process

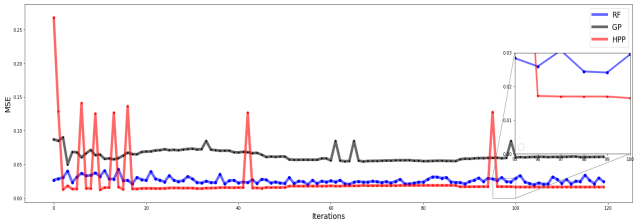

FIGURE 9. MSE in 9D.

TABLE 3. MSE in 9D.

iterations	1	5	10	25	50	100
HPP	0.26761	0.01879	0.01887	0.01701	0.01653	0.01656
RF	0.02663	0.02728	0.03310	0.02679	0.02344	0.02546
GP	0.08707	0.08606	0.06474	0.07189	0.05852	0.06298

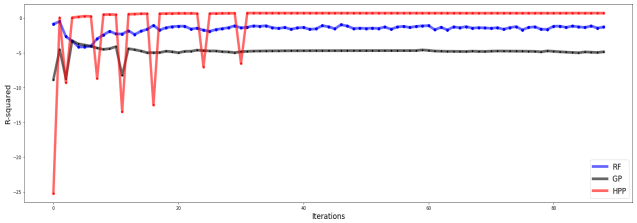

FIGURE 10. R-Squared in 2D.

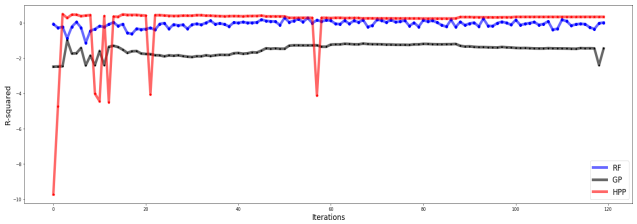

FIGURE 11. R-Squared in 9D.

of the GP sometimes fails, resulting in a large error, as shown in Fig. 9.

After the MSE metric has stabilized during the iteration process, the GP is much higher than the RF and HPP, and the result of the GP presents a large increase, as shown in Table 3. In contrast, the increase in the input dimension has minimal effect on the MSEs of the RF and HPP models. The HPP's MSE is two-thirds that of the RF, and the HPP's MSE is one-fifth that of the GP on average.

b: R-SQUARED

The R-Squared is an alternative index describing the accuracy of the model. This indicator evaluates the representation and descriptiveness of the model for heterogeneous systems with a score of between 0 and 1. The closer the index is to 1, the better the performance.

The R-Squared in two different cases are shown in Fig. 10 and Fig. 11, and the HPP's R-Squared for the system is better than the other surrogate model in both situations.

TABLE 4. R-Squared in 2D.

iterations	1	2	5	10	30	50
MSP	-25.218	0.0277	0.1649	0.5185	0.6614	0.7055
RF	0.0607	0.2764	-1.7044	-0.7925	-0.2648	-0.1662
GP	-25.216	-0.4206	-1.5523	-0.4801	0.0553	0.1281

TABLE 5. R-Squared in 9D.

iterations	1	5	10	25	50	100
MSP	-4. 3271	0. 46249	0.35158	0.40518	0.33797	0.50109
RF	-3.37263	-0.08223	0.00716	0.11835	0.04298	0.11216
GP	-2.48856	-1.72294	-1.77420	-1.18564	-1.49012	-1.52631

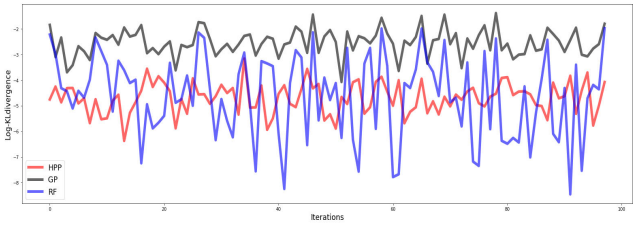

FIGURE 12. KLdivergence in 9D.

Similar to the MSE results, Fig. 11 and Table 4 indicate that the primitive RF and GP are not applicable for the representation of a multimodal heterogeneous network with strong randomness.

For the high-dimensional scenario, Table 5 shows that the RF and GP are completely ineffective, whereas the fitting performance of HPP is still acceptable.

c: KL AND JS-DIVERGENCE

Here, we compare the probability distribution similarity between the agent model and actual observation statistics. The Kullback-Leibler divergence (KL divergence) is a method for describing the difference between two probability distributions. Intuitively, it can be used to measure the degree to which a given arbitrary distribution deviates from the actual distribution. The Jensen-Shannon divergence (JS divergence), also known as the JS distance, is a variant of the KL divergence. In comparison to the KL divergence, the JS divergence can be regarded as a generalized distance measure with symmetry.

The logarithms of the Kl divergence and JS divergence and their mean and variance for the iterative statistics in the 9D case are shown in Fig. 12 and Fig. 13. The mean value of the model gradually converges after repeated iterations. The mean jitters of the GP and HPP are very similar, and the deviations are very small. However, the KL degree of similarity of the probability is more than ten times that of the GP. From the model stability perspective, the performance of the RF in expressing the multimodal distribution is similar to the HPP but with larger errors.

The JS divergence of the GP and HPP shows the same characteristics as their KL divergence. As shown in Fig. and

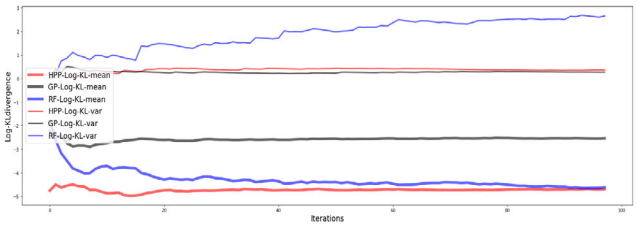

FIGURE 13. KLdivergence features in 9D.

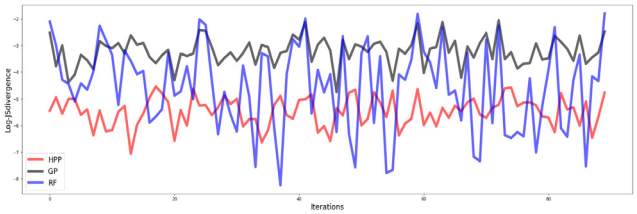

FIGURE 14. JSdivergence in 9D.

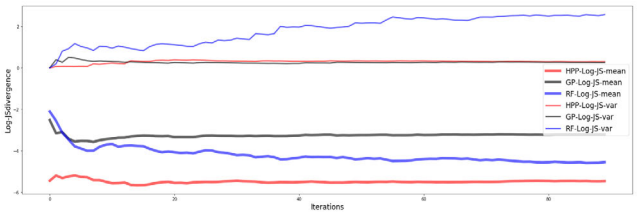

FIGURE 15. JSdivergence features in 9D.

Fig., the distribution similarity of the RF performance in the JS divergence is worse, while the mean of the JS of RF increases to being between that of HPP and GP. We further explain the instability of the RF estimation and prediction in the scenario with this multimodal feature.

Under the model generalized representation capacity condition, Bayesian optimization based on the HPP is significantly better than the other surrogate model in terms of the ability for the fine-grained uncertainty expression in this type of heterogeneous network scheme with a statically multimodal observation distribution.

4) COMPARISON OF METHOD CRITERIONS

In this chapter, we compare different surrogate model and acquisition function combinations in the 9D parameters with the same hyperparameters τ in the Martern kernel and β of the UCB for the methods. To compare the optimization performance of the strategy-model combination with multiple K, we depart from the ideal situation to obtain the reference design combination and the difference of evaluated observation and model prediction for the comparison.

a: HYPERPARAMETER SENSITIVITY TEST

In the WDUCB, we adjust the hyperparameters K in the criterion to compare the effect of K on the acquisition function

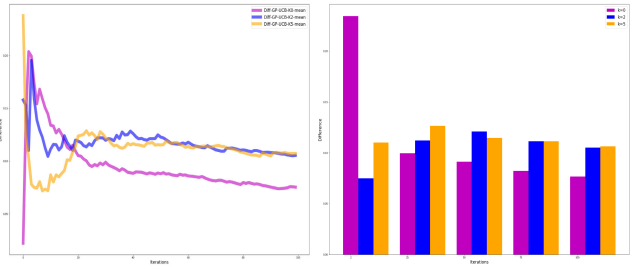

FIGURE 16. GP-UCB difference in multiple K.

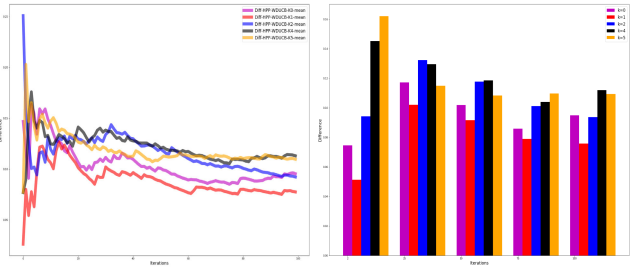

FIGURE 17. HPP-WDUCB difference in multiple K.

strategy in the same iteration number with the same surrogate model in scenario.

The GP-UCB and HPP-WDUCB cases are shown in Fig. 16 and Fig. 17. Here, we introduce the linear attenuation factor. In the case of a loss function with uncertain design parameters, we set the iteration time as the termination condition and linear decay the K value each iteration.

Obviously, compared with GP-UCB, the influence of K in HPP-WDUCB on iterations is less after adding attenuation factor. During the comparison, the difference between the multiple K values converges. Statistical results that the influence of K is more reflected in the second-order difference, which still affects the selection of the exploration strategy and the speed of policy conversion in the WDUCB. In the heterogeneous network tuning, the attenuation factor can guarantee the criterion convergence of the iteration process. It provides a realistic reference for practical scenarios.

In the next subsection, we compare and demonstrate the iteration behavior for a series of BO method combinations.

b: OPTIMIZATION PATH COMPARISON

A preliminary criterion optimization path comparison is evaluated between GP-UCB and HPP-WDUCB with the same K and β. The comparison focuses on the predicted query point sequence and criterion corresponding to each surrogate model's prediction, and the evaluated observations of scenario are simulated. The difference between the predicted value and the actual simulated feature reflects the transformation of the strategy in the iterative process to a certain extent.

The results of 60 iterations comparisons are drawn in Fig. 18. The red solid line represents the prediction-simulation differences of the HPP-WDUCB. The black solid

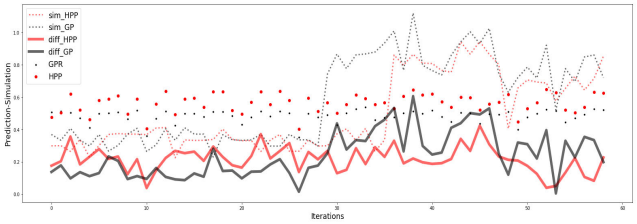

FIGURE 18. Statistics of GP-UCB and HPP-WDUCB.

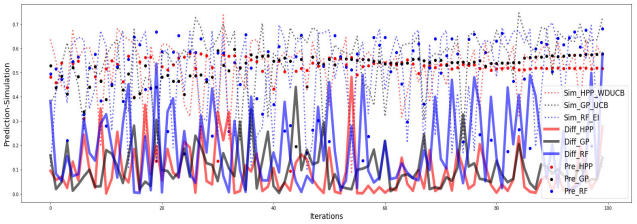

FIGURE 19. Statistics for GP-UCB,HPP-WDUCB,RF-EI.

TABLE 6. Prediction differences over iterations.

iterations	10	20	30	40	50	60
HPP-WDUCB	0.21617	0.17882	0.26753	0.19684	0.20785	0.08273
GP-UCB	0.11182	0.14609	0.25245	0.29784	0.31899	0.33394

line is the difference for the GP-UCB. As a standard, the GP-UCB performs exploration in the first half of the iteration with a smaller difference before the query point reached the optimal range of the hypercube. In contrast to the GP-UCB, the HPP-WDUCB method attempts more exploration processes during the earlier iterations, and then, the WDUCB's attenuation factor tunes the exploration strategy to an exploitation strategy with higher accuracy.

The preliminary prediction difference is shown in Table 6, where the exploration of GP-UCB's prediction is more negative than that of HPP-WDUCB in the first step. And after a series of attempts, the prediction-simulation difference of HPP-WDUCB is 34% lower than GP-UCB on average, which shows that the HPP-WDUCB performance is better than GP-UCB in the exploitation phase.

c: METHOD COMBINATION APPRAISAL

In a high-dimensional scenario, we generally analyze the application of various models and acquisition strategies combinations.

First we enumerate a variety of different optimization method combinations to 100 iteration experiments. As a generally applicable strategy, the HPP-WDUCB with the multiple k, and the EI criterion is added to the Random Forest model (RF-EI). The raw statistics for GPR-UCB, HPP-WDUCB and RF-EI are drawn in Fig. 19.

It is difficult to distinguish the preliminary statistics due to the query path of the optimization process for each combination is different, and the strategic change in the acquisition criterion simultaneously leads to the strong jitter of the evaluation difference as shown in Fig. 19.

Thus, we calculate the difference for each combination of raw results and obtain the more visible results in Fig. 20. And we compare the reference combinations of design indicators with all the method process. In general, under the 95% confidence, the results shown in Fig. 20 by blue,yellow and purple lines are the performances of HPP-WDUCB in K=0,2 and GP-UCB in K=2 are in line with expectations after few iterations.

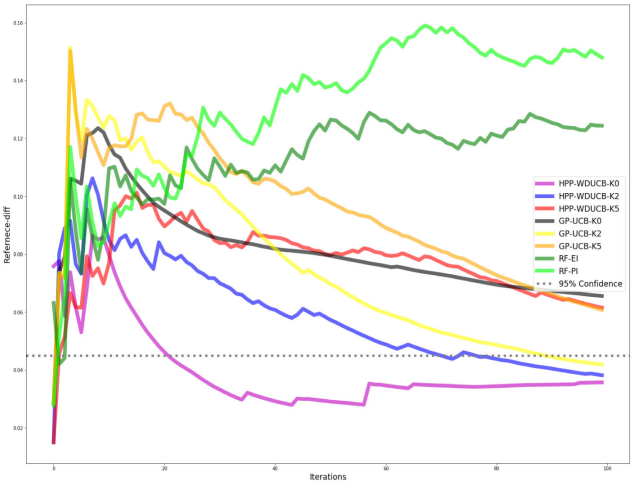

FIGURE 20. Reference simulation-prediction statistics.

But due to the multiple path of optimization method in the high-dimensional hyperspace in heterogeneous networks, the uncertainties in complex application cannot be ignored. It seems to be impossible to identify a "winner" among the proposed approaches; however, some relevant insights can be obtained from the iteration process.

1) The RF-PI is similar to the RF-EI result. RF itself has poor expressive ability in this multimodal feature distribution system with sparse observations, especially in the case of a high-dimensional scenario. The difference between the prediction and simulation is mainly caused by the error in the prediction, as seen in the EI criterion. There is no reduction in the error as the iteration progresses in the RF-EI strategy.

2) In the GP-UCB combination, the target of the criterion is seriously affected by K. We compare three different K values (K=0, 2, 5). Initially, the GP-UCB methods based on different K also show a large difference in the search path. After approximately halfway through the iteration process, the difference converges in multiple rates. And the speed of convergence is also strongly affected by the parameters of the complex network and the focus of the exploration-exploitation process. The hyperparameters need to be carefully adjusted in order to produce good optimization results for specific scenarios.

3) In the proposed HPP-WDUCB combination, the trend is similar to GP-UCB. As a multimodal extension of the hybrid stochastic process model, the HPP shows great expressive

characteristics. And the HPP-WDUCB is parameter insensitive, it follows the strategy of exploration in the iteration process. The change of strategy will not be greatly affected by the problem of parameter setting. In the end, a satisfactory approximate optimal result can be obtained. Because of the complex structure of the HPP, it is necessary to add subjective evaluation strategies to specific scenarios to achieve the desired quantitative optimal design combination.

V. CONCLUSION

In this paper, we proposed a novel Bayesian optimization method with a generalized hybrid probability process (HPP) model and a model-fitting weight degenerate upper confidence bound (WDUCB) acquisition criterion for multimodal heterogeneous network model representation and orchestration. The method is adapted to scenarios for 5G and beyond space heterogeneous network multi-service scenarios, and the comparison results obtained by the proposed HPP-WDUCB model with the criterion reveal an impressive performance in heterogeneous network representation and optimization. The application cases illustrate that the hybrid probability process significantly improves the stability of the model representation and outperforms the exact Gaussian process and random forest in terms of accuracy and interpretability. The HPP-WDUCB combination provides a novel parameter-insensitive exploration-exploitation approach generalized to fuzzy observations as a credible data-driven reference for the top-level design of orchestration of current multimodal heterogeneous network.

Furthermore, due to the lack of a real configurable network system and the reality that large-scale heterogeneous network convergence does not have a unified optimal standard, the proposed method is currently applicable to the verification of network design simulations and requires an existing network. However, the Bayesian optimization with hybrid probability process demonstrates a wide range of future application scenarios for heterogeneous network orchestration.

REFERENCES

[1] S. Onoe, "1.3 evolution of 5G mobile technology toward 1 2020 and beyond," in *IEEE ISSCC Dig. Tech. Papers*, Jan./Feb. 2016, pp. 23–28.
[2] B. Shahriari, K. Swersky, Z. Wang, R. P. Adams, and N. de Freitas, "Taking the human out of the loop: A review of Bayesian optimization," *Proc. IEEE*, vol. 104, no. 1, pp. 148–175, Jan. 2016.
[3] Z. Ghahramani, "Probabilistic machine learning and artificial intelligence," *Nature*, vol. 521, no. 7553, pp. 452–459, 2015.
[4] H. Q. Tran, C. Van Phan, and Q.-T. Vien, *Emerging Wireless Communication and Network Technologies*. Singapore: Springer, 2018.
[5] T. Rings, G. Caryer, J. Gallop, J. Grabowski, T. Kovacikova, S. Schulz, and I. Stokes-Rees, "Grid and cloud computing: Opportunities for integration with the next generation network," *J. Grid Comput.*, vol. 7, no. 3, pp. 375–393, 2009.
[6] S. Khara, I. S. Mishra, and D. Saha, "Global gateway-based UMTS/WLAN integration for improved delay performance," *Int. J. Parallel, Emergent Distrib. Syst.*, vol. 25, no. 2, pp. 153–170, 2010.
[7] B. Ahlgren, L. Eggert, B. Ohlman, and A. Schieder, "Ambient networks: Bridging heterogeneous network domains," in *Proc. IEEE 16th Int. Symp. Pers., Indoor Mobile Radio Commun.*, Sep. 2005, pp. 937–941.
[8] J. F. Monserrat, G. Mange, V. Braun, H. Tullberg, G. Zimmermann, and Ö. Bulakci, "METIS research advances towards the 5G mobile and wireless system definition," *EURASIP J. Wireless Commun. Netw.*, vol. 2015, no. 1, p. 53, Mar. 2015.
[9] X. Zhang, Y. Zhang, R. Yu, W. Wang, and M. Guizani, "Enhancing spectral-energy efficiency for LTE-advanced heterogeneous networks: A users social pattern perspective," *IEEE Wireless Commun.*, vol. 21, no. 2, pp. 10–17, Apr. 2014.
[10] M. Jo, T. Maksymyuk, R. L. Batista, T. F. Maciel, A. L. F. D. Almeida, and M. Klymash, "A survey of converging solutions for heterogeneous mobile networks," *IEEE Wireless Commun.*, vol. 21, no. 6, pp. 54–62, Dec. 2014.
[11] S. Kittiperachol, Z. Sun, and H. Cruickshank, "Performance evaluation of on-board QoS support for multiservice applications on the integrated next generation satellite-terrestrial network," in *Proc. 4th Adv. Satell. Mobile Syst. (ASMS)*, Aug. 2008, pp. 311–316.
[12] A. Guidotti, A. Vanelli-Coralli, M. Conti, S. Andrenacci, and S. Cioni, "Architectures and key technical challenges for 5G systems incorporating satellites," *IEEE Trans. Veh. Technol.*, vol. 68, no. 3, pp. 2624–2639, Mar. 2019.
[13] J. L. Walker and C. Hoeber, "Technical challenges of integration of space and terrestrial systems," in *Handbook of Satellite Applications*. Cham, Switzerland: Springer, 2015.
[14] D. Li, X. Shen, D. Li, and S. Li, "On civil-military integrated space-based real-time information service system," *Geomatics Inf. Sci. Wuhan Univ.*, vol. 42, pp. 1501–1505, Feb. 2017.
[15] D. A. Temesgene, J. Núñez-Martínez, and P. Dini, "Softwarization and optimization for sustainable future mobile networks: A survey," *IEEE Access*, vol. 5, pp. 25421–25436, 2017.
[16] M. M. Mowla, I. Ahmad, D. Habibi, and Q. V. Phung, "A green communication model for 5G systems," *IEEE Trans. Green Commun. Netw.*, vol. 1, no. 3, pp. 264–280, Sep. 2017.
[17] R. Li. (2018). *Network 2030: Market Drivers and Prospects*. Accessed: Oct. 2, 2018. [Online]. Available: https://www.itu.int/en/ITU-T/Workshops-and-Seminars/201810/Documents/
[18] H. P. Vanchinathan, I. Nikolic, F. De Bona, and A. Krause, "Explore-exploit in top-N recommender systems via Gaussian processes," in *Proc. 8th ACM Conf. Recommender Syst.*, 2014, pp. 225–232.
[19] J. Snoek, O. Rippel, K. Swersky, R. Kiros, N. Satish, N. Sundaram, M. Patwary, M. Prabhat, and R. Adams, "Scalable Bayesian optimization using deep neural networks," in *Proc. Int. Conf. Mach. Learn.*, 2015, pp. 2171–2180.
[20] J. T. Springenberg, A. Klein, S. Falkner, and F. Hutter, "Bayesian optimization with robust Bayesian neural networks," in *Proc. Adv. Neural Inf. Process. Syst.*, 2016, pp. 4134–4142.
[21] Y. Zhang, K. Sohn, R. Villegas, G. Pan, and H. Lee, "Improving object detection with deep convolutional networks via Bayesian optimization and structured prediction," in *Proc. IEEE Conf. Comput. Vis. Pattern Recognit.*, Jun. 2015, pp. 249–258.
[22] N. Mahendran, Z. Wang, F. Hamze, and N. De Freitas, "Adaptive MCMC with Bayesian optimization," in *Proc. 13th Int. Conf. Artif. Intell. Statist.*, 2010, pp. 751–759.
[23] R. Martinez-Cantin, "BayesOpt: A Bayesian optimization library for nonlinear optimization, experimental design and bandits," *J. Mach. Learn. Res.*, vol. 15, no. 1, pp. 3735–3739, 2014.
[24] Z. Wang, B. Shakibi, L. Jin, and N. de Freitas, "Bayesian multi-scale optimistic optimization," in *Proc. 17th Int. Conf. Artif. Intell. Statist.*, 2014, pp. 1005–1014.
[25] Y. Xia, C. Liu, Y. Li, and N. Liu, "A boosted decision tree approach using Bayesian hyper-parameter optimization for credit scoring," *Expert Syst. Appl.*, vol. 78, pp. 225–241, Jul. 2017.
[26] A. Klein, S. Falkner, S. Bartels, P. Hennig, and F. Hutter, "Fast Bayesian optimization of machine learning hyperparameters on large datasets," 2017, *arXiv:1605.07079*. [Online]. Available: https://arxiv.org/abs/1605.07079
[27] T. Zhang, Q. Zhao, K. Shin, and Y. Nakamoto, "Bayesian-optimization-based peak searching algorithm for clustering in wireless sensor networks," *J. Sens. Actuator Netw.*, vol. 7, no. 1, p. 2, 2018.
[28] A. Candelieri, R. Perego, and F. Archetti, "Bayesian optimization of pump operations in water distribution systems," *J. Global Optim.*, vol. 71, no. 1, pp. 213–235, 2018.
[29] M. Garnelo, D. Rosenbaum, C. J. Maddison, T. Ramalho, D. Saxton, M. Shanahan, Y. W. Teh, D. J. Rezende, and S. M. A. Eslami, "Conditional neural processes," 2018, *arXiv:1807.01613*. [Online]. Available: https://arxiv.org/abs/1807.01613

[30] M. Przygrodzki and W. Lubicki, "Use of LHS sampling to calculate probabilistic power flow," *Acta Energetica*, pp. 189–196, 2017.
[31] E. Snelson and Z. Ghahramani, "Sparse Gaussian processes using pseudo-inputs," in *Proc. Int. Conf. Neural Inf. Process. Syst.*, 2006, pp. 1257–1264.
[32] N. Srinivas, A. Krause, S. M. Kakade, and M. W. Seeger, "Information-theoretic regret bounds for Gaussian process optimization in the bandit setting," *IEEE Trans. Inf. Theory*, vol. 58, no. 5, pp. 3250–3265, May 2012.
[33] N. Srinivas, A. Krause, S. Kakade, and M. Seeger, "Gaussian process optimization in the bandit setting: No regret and experimental design," in *Proc. 27th Int. Conf. Int. Conf. Mach. Learn.*, 2009, vol. 58, no. 5, pp. 1015–1022.
[34] X. Xie and K. Chen, "An AHP-based evaluation model for service composition," in *Computational Science and Its Applications—ICCSA*, M. L. Gavrilova, O. Gervasi, V. Kumar, C. J. K. Tan, D. Taniar, A. Laganá, Y. Mun, and H. Choo, Eds. Berlin, Germany: Springer, 2006, pp. 756–766.

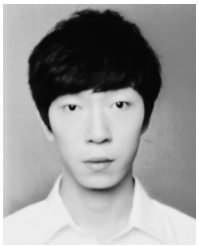

HAI WANG received the B.Eng. degree in communication engineering in communication and information systems from Wuhan University, China, in 2014, where he is currently pursuing the Ph.D. degree. His research interests include wireless communication networks, edge computing, and network optimization.

GENG ZHANG received the B.Eng. degree in communication engineering in communication and information systems from Xidian University, China, in 2010. He is currently a Senior Engineer with the China Electric Power Research Institute. He has authored over 20 papers in different journals and conferences. His research interest includes electric power communication networks.

HAO JIANG received the B.Eng. degree in communication engineering and the M.Eng. and Ph.D. degrees in communication and information systems from Wuhan University, China, in 1999, 2001, and 2004, respectively. From 2004 to 2005, he undertook his postdoctoral research work at LIMOS, Clermont-Ferrand, France. He was a Visiting Professor with the University of Calgary, Canada, ISIMA, and Blaise Pascal University, France. He is currently a Professor with Wuhan University. He has authored over 60 papers in different journals and conferences. His research interests include mobile ad hoc networks and mobile big data.

JING WU received the B.Eng. degree in communication engineering and the Ph.D. degree in communication and information systems from Wuhan University, China, in 2002 and 2007, respectively. From 2004 to 2005, she undertook her postdoctoral research work at LIMOS, Clermont-Ferrand, France. She is currently an Associate Professor with Wuhan University. Her research interests include wireless communication networks, network simulation, and intelligence data processing.

XING YANG received the B.Eng. degree in communication engineering from Lanzhou University, China, in 2016. He is currently pursuing the M.Eng. degree with Wuhan University, China. His research interests include wireless communication, network model and simulation, and machine learning.

MO ZHOU received the B.Eng. degree in communication engineering from Wuhan University, China, in 2018, where she is currently pursuing the master's degree in electronics and communication engineering. She recently participates in project research about evaluation of simulation data and has implemented four evaluation algorithms.